2007 IEEE International Conference on
Robotics and Automation
Roma, Italy, 10-14 April 2007



# The design of a tethered aerial robot

Phillip J. M[c]Kerrow, *Member, IEEE* and Danny Ratner

*Abstract*—**This paper describes the design and modeling of a robot that swings on the end of a tether. Its height above the ground is controlled by the length of the tether. Its location on a spherical shell at the end of the tether is controlled by a pair of ducted fans. The vertical orientation of its body is determined by the point at which the horizontal thrust force acts relative to the centre of gravity (cog).**

**The system acts like a double pendulum with two modes of natural movement. It is modeled with coordinate frames at the ends of the tether and at the cog. Due to the second mode of motion it may oscillate around its centre of gravity while it swings or flies in a circle. From the dynamic model we develop a model for simulating the motion of the tethered robot.**

## I. Introduction

MANY research groups are developing aerial robots for security and rescue operations [1, 2]. The problems posed by urban search and rescue are very difficult [3, 4]. No mater whether a system is designed to inspect the outside of a building or search for casualties in a disaster, its goal is to fly sensors into a difficult to-get-to site and send back video and audio information to a remote operator.

Researchers are developing systems with both traditional and novel aircraft. Each aircraft type has its advantages and disadvantages. Each approach has to achieve a balance between stability in flight and maneuverability in close environments. They have to provide stable sensing platforms without crashing [5].

Some are experimenting with fixed wing airplanes [6], others with blimps and others with helicopters [7]. A manually flown helicopter has the problem that if its rotor blades clip an object then the helicopter crashes [8]. Others are experimenting with novel flight platforms including bird like robots with flapping wings [9] and kites [10].

In this paper, we introduce a different type of flying robot: a robot that swings on the end of a tether. In a previous paper [1], we described the concepts, potential applications and problems of building a tethered robot. In this paper, we describe the design of a robot that swings on the end of a tether.

A tethered robot can be lowered from the top of a building to inspect the side of the building or to peer into windows. It can be lowered down a vertical shaft, such as a mine air supply shaft, to look for people trapped behind a rock fall. It can be lowered from a helicopter hovering over a village to reconnoiter between buildings.

The above applications inspired the development of this robot. The advantage of lowering a robot on a tether, rather than just a sensor, is that the robot can maneuver around obstacles as it is driven to inspect a remote object.

Tethers are commonly used with underwater robots [11] for remote tele-operation, to provide power and communications and to avoid losing the robot. Tethers have been used on walking robots to enable those robots to enter dangerous areas, such as the inside of a volcano [12]. Tethers have also been proposed for controlling robots in space [13]. Previous swinging robots have been monkey like robots with two hands to grasp a wire [14].

Controlling a robot swinging on the end of a tether presents interesting control problems for research. A helicopter robot can move in 6 degrees of freedom (dof) and is marginally stable in each of those degrees. When hovering and at low speeds there is no friction or damping due to wind flow over the vehicle, so the only source of force to oppose motion is inertia.

The tether on a tethered robot constrains its motion in 5 of the 6 degrees of freedom. The only degree that is not constrained is yaw, as the robot is free to rotate around the axis of the tether. In practice the weight of the robot creates tension in the tether that can cause some resistance to turning, particularly when the tether is a braided cord. The tether we use is a high strength (50Kg) monofiliment fishing line, so the robot is free to yaw.

These constraints on motion create two other reasons for building this robot. One is to experiment with various algorithms for controlling yaw. As the yaw axis is unconstrained, its dynamics will be similar to the yaw axis of a free flying helicopter, except we can't crash it. Another application is the simulation of the motion of a helicopter for research into visual servoing [15]. In the following sections, we discuss the design and modeling of this robot.

## II. Swinging robot concept

We started with a drink bottle hanging on a string (Fig. 1.). The water in the bottle moved the cog toward the bottom. In the stationary position, the vertical force due to gravity acting through the cog is balanced by a tension force in the tether. When a horizontal force is applied through the cog by the fans, the bottle swings away from the vertical, and the bottle and tether are at the same angle to the vertical. If the force is reduced to zero the bottle swings like a simple pendulum around the point where the tether is attached to the ceiling.

Manuscript received September 15, 2006.

P. J. McKerrow is with the University of Wollongong, Wollongong, NSW 2522 AUSTRALIA (phone: +612 4221 3771; fax: +612 4221 4170; e-mail: phillip@ uow.edu.au).

D. Ratner, was with the University of Wollongong, Wollongong, NSW 2522 AUSTRALIA (e-mail: danny_ratner@yahoo.com.au).

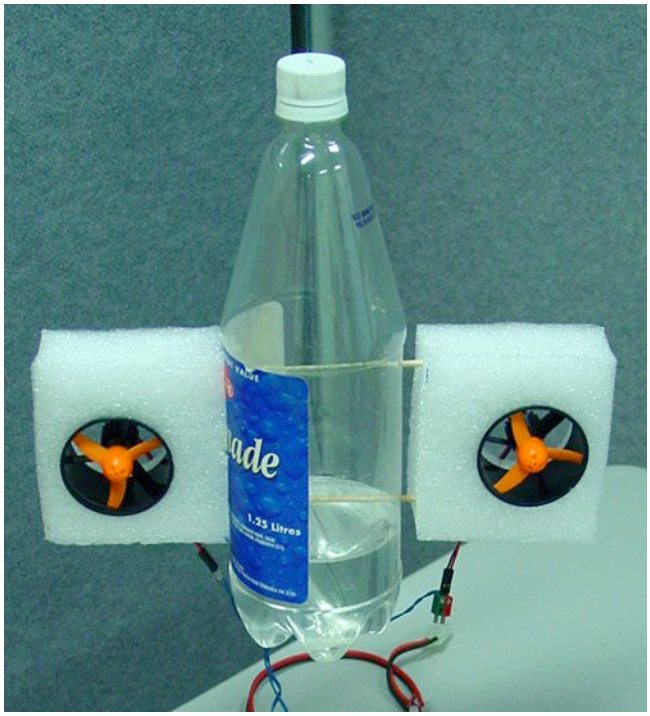

Fig. 1. Drink bottle used to test initial ideas.

The effect of the tether is to provide a spring force in 5 of the 6 degrees of freedom that returns the robot to the no power position. Yaw is not constrained by the tether. Minor twist forces in the tether are minimized by the rotary hinge joint at the top of the robot.

When the fans are moved higher, so that the thrust force is applied above the cog the bottle tilts less than the tether. In inspection tasks it is desirable to have the robot oriented close to vertical at all swing angles to cause the least disturbance to any sensors that are attached. However, the cost is that when the force is reduced to zero the bottle swings with two modes of oscillation: one around the tether point as above and one around the cog. The later has a higher frequency.

## III. Robot Design

We built the robot from a length of plastic pipe (Fig. 2.). The robot is attached to a 50Kg breaking strain mono-filament (fishing line) with a swivel that contains a ball bearing. Also, the attachment ring is free to rotate. The ducted fans are placed toward the top of the robot with their H-Bridge amplifiers and controllers in the tube above them.

The heaviest items are the batteries, so they are placed toward the bottom of the tube. Three batteries are used, partly due to different components having differing voltage requirements and partly to separate power and control circuits to reduce interference. One powers the ducted fans, one powers the servos in the pan and tilt unit and one powers the computer and the sensors.

The volume between the batteries and the power switches houses the control computer and the sensors.


Fig. 2. Tethered robot swinging from the ceiling.

The computer is a Parallax Basic Stamp (Fig. 3.). Its limitations are that it can only run one process at a time and its serial i/o is not buffered. Its advantage is that it is simple to program. If the Basic Stamp proves to be inadequate we will replace it with a Java based microcontroller that supports multi-processing.

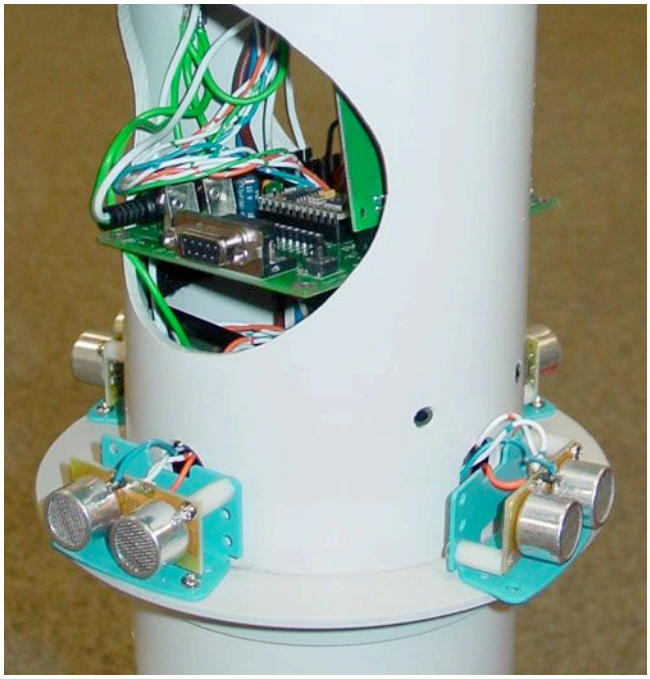

Fig. 3. Basic Stamp computer (horizontal) located above sensor suite.

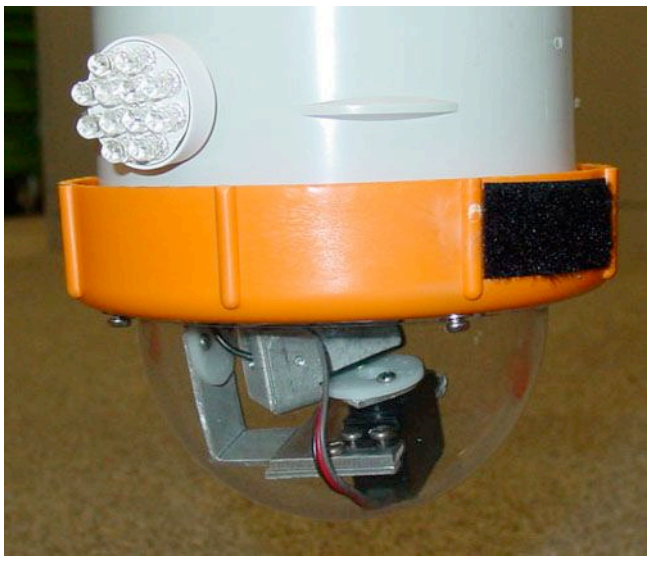

Fig. 4. Payload is a spy camera mounted on a pan-and-tilt unit in a clear hemisphere at the bottom of the robot.

The sensor suite includes several ultrasonic range sensors to measure range and angle to walls, a two-axis inclinometer to measure tilt angle components, a magnetometer to measure bearing, and an inertial navigation sensor INS to measure yaw rate. Forward-looking ultrasonic sensors and tilt will be used to control the magnitude of the swing. The INS, or the magnetometer, or pairs of ultrasonic sensors will be used to control the direction of the swing.

In addition to the sensors used for control, the robot carries a video (spy) camera as a payload (Fig. 4.). This camera is located in a transparent hemisphere at the bottom of the robot. It is mounted on a pan and tilt unit made from radio-control model servos. Its purpose is to send video images back to the user of the robot. The user will drive the robot to the location that he desires to inspect and turn the spy camera to view the area.

The angle to which the robot can swing is determined by the weight of the robot and the force that can be applied by the ducted fans. The distance that it swings from the vertical is determined by the maximum swing angle and the length of the tether. In the laboratory (Fig. 2.). The distance to the roof is small so it doesn't swing very far. The plastic pipe is thick so the weight is considerable.

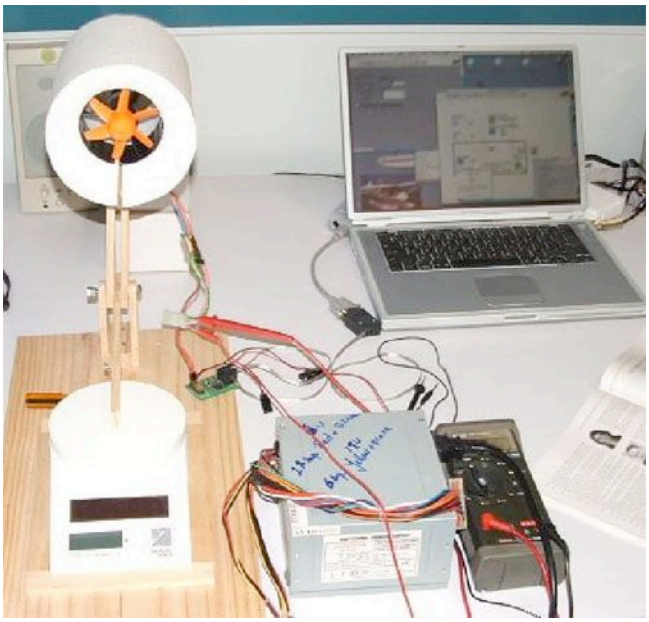

Fig. 5. Test rig to measure thrust of ducted fan.

To measure the trust of the ducted fans we constructed a test rig (Fig. 5.). The rig converts the horizontal force produced by the fan to a vertical force on the electronic weight scale. We can measure force relative to revolutions per minute and relative to motor voltage.

## IV. Robot Model

The kinematic model of the robot consists of three coordinate frames (Fig. 6.): a reference fame (**W**) located at the point where the tether attaches to the support structure, a tether frame (**T**) at the point where the tether attaches to the robot, and a robot frame (**R**) located at the cog of the robot. Each frame is internal to the object it is attached to, and the succeeding frame moves within it. For example the tether frame (**T**) is fixed at the distal end of the tether with its z axis collinear with the tether. As a result, the tether frame (**T**) moves in the reference frame (**W**), and the robot frame (**R**) moves in the tether frame (**T**).

This is potentially a roll-roll system, so we chose to assume that all rotation around the z axis occurs in the tether and not in the hinge between the tether and robot. Consequently, the y axes of the robot and tether frames are parallel, so the robot frame has only one angular degree of freedom (dof) relative to the tether frame: y rotation (pitch).

When no power is applied to the motors the robot hangs directly below the hinge point with the tether coincident with

the z axis of the reference frame (**W**), as shown in Fig. 6. When power is applied to the motors the resultant thrust swings the robot out away from this z axis and flies the robot in a circular path around it. To hold the robot in a stationary swing position the motor thrust vector must intersect the z axis of the reference frame.

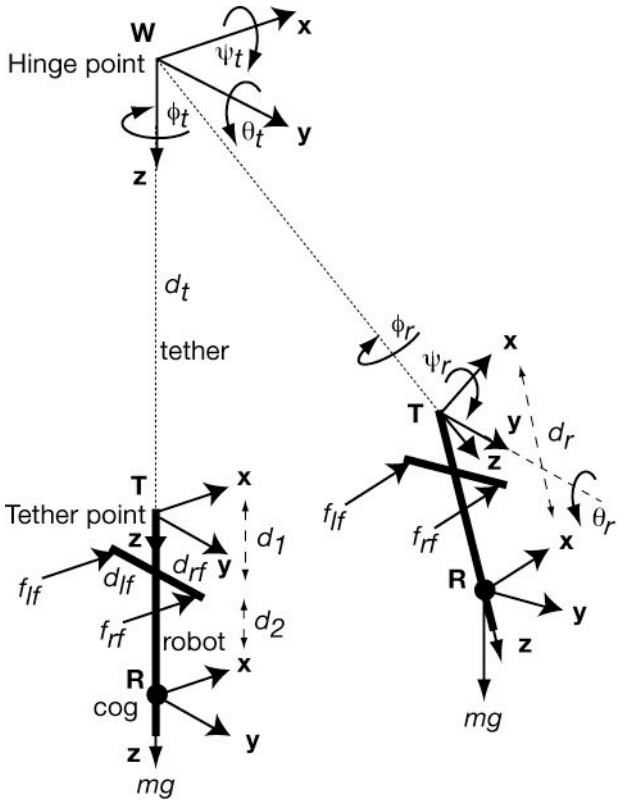


Fig. 6. Location of forces and coordinate frames used in model.

Three forces are applied to the robot: two fan forces ($f_{lf}$ and $f_{rf}$) and the force due to gravity ($mg$). Gravity acts in the z direction with respect to the reference frame.

$$ {}^{W}f_g = \begin{bmatrix} 0 \\ 0 \\ mg \end{bmatrix} = {}^{W}T_T\,{}^{T}T_R\,{}^{R}f_g = {}^{W}T_R\,{}^{R}f_g \tag{1} $$

where the transform from the reference to the tether frame is (yaw, pitch, roll, translate):

$$ {}^{W}T_T = Rot(z,\phi_t)Rot(y,\theta_t)Rot(x,\psi_t)Trans(z,d_t) \tag{2} $$

where $(\psi_t,\theta_t,\phi_t)$ is the angle of the tether and $d_t$ is its length, and the rotation transform is:

$$ \begin{aligned} {}^{W}Rot_R &= Rot(z,\phi)Rot(y,\theta)Rot(x,\psi) \\ &= \begin{bmatrix} C\phi C\theta & C\phi S\theta S\psi - S\phi C\psi & C\phi S\theta C\psi + S\phi S\psi \\ S\phi C\theta & S\phi S\theta S\psi + C\phi C\psi & S\phi S\theta C\psi - C\phi S\psi \\ -S\theta & C\theta S\psi & C\theta C\psi \end{bmatrix} \end{aligned} \tag{3} $$

As force is a vector, the transformation from the reference frame to the robot frame (Eqn. 3.) is the rotation component of the general transform in 3D space [16], where the angle of the robot is the sum of the angle of the tether relative to the reference frame and the angle of the robot relative to the tether frame:

$$ \begin{aligned} \psi &= \psi_t + \psi_r = \psi_t + 0 = \psi_t \\ \theta &= \theta_t + \theta_r \\ \phi &= \phi_t + \phi_r = \phi_t + 0 = \phi_t \end{aligned} \tag{4} $$

In the robot frame the force due to gravity is:

$$ \begin{aligned} {}^{R}f_g &= {}^{W}Rot_R^{-1}\,{}^{W}f_g \\ &= \begin{bmatrix} C\phi C\theta & S\phi C\theta & -S\theta \\ C\phi S\theta S\psi - S\phi C\psi & S\phi S\theta S\psi + C\phi C\psi & C\theta S\psi \\ C\phi S\theta C\psi + S\phi S\psi & S\phi S\theta C\psi - C\phi S\psi & C\theta C\psi \end{bmatrix} \begin{bmatrix} 0 \\ 0 \\ mg \end{bmatrix} \\ &= \begin{bmatrix} -mgS\theta \\ mgC\theta S\psi \\ mgC\theta C\psi \end{bmatrix} = \begin{bmatrix} {}^{R}f_{gx} \\ {}^{R}f_{gy} \\ {}^{R}f_{gz} \end{bmatrix} \end{aligned} \tag{5} $$

Notice, that rotation around the z axis ($\phi$) has no impact on the gravitational force in the robot frame. The fan forces act in the x direction with respect to the robot frame, and

$$ {}^{R}f_{lf} = \begin{bmatrix} f_{lf} \\ 0 \\ 0 \end{bmatrix} \tag{6} $$

### *A. Force Balance*

The static model of the robot is the force balance at the cog. First, we replace the fan forces by equivalent forces through the cog and torques around the cog.

$$ {}^{R}f_{fans} = \begin{bmatrix} f_{lf} + f_{rf} \\ 0 \\ 0 \end{bmatrix} \tag{7} $$

$$ {}^{R}\tau_{fans} = \begin{bmatrix} 0 \\ -(f_{lf} + f_{rf})d_2 \\ f_{lf}d_{lf} - f_{rf}d_{rf} \end{bmatrix} \tag{8} $$

Second, we transform the force in the tether into the robot frame. The force in the tether consists of two components: a tension force along the z axis of the tether frame, that holds the robot up in the air, and a very small torque around the z axis due to twist in the tether. It is this tether force that constrains the motion of the robot in 5 of the 6 dof.

Any torque due to the twist of the cable will oppose yaw motion and hence constrain motion in the 6th dof. At present we will ignore it, assuming it places no constraint on yaw.

Also, we will ignore the elasticity of the tether, which will cause it to increase in length slightly when carrying the weight of the robot. Also, we assume that the tether is straight.

$$ {}^{R}f_{teth} = {}^{T}Rot_{R}^{-1}\,{}^{T}f_{teth} = {}^{T}Rot_{R}^{-1}\begin{bmatrix}0\\0\\-f_{teth}\end{bmatrix} = \begin{bmatrix}f_{teth}S\theta_r\\-f_{teth}C\theta_r S\psi_r\\-f_{teth}C\theta_r C\psi_r\end{bmatrix} $$
$$ = \begin{bmatrix}f_{teth}S\theta_r\\-f_{teth}C\theta_r * 0\\-f_{teth}C\theta_r 1\end{bmatrix} = \begin{bmatrix}f_{teth}S\theta_r\\0\\-f_{teth}C\theta_r\end{bmatrix} = \begin{bmatrix}{}^{R}f_{tethx}\\{}^{R}f_{tethy}\\{}^{R}f_{tethz}\end{bmatrix} \quad (9) $$

Third, we replace the force in the tether with an equivalent force through the cog and torque around the cog. To calculate the torque, we multiply the force vector by the length of the normal to the force vector from the cog. As we have transformed the force vector into the robot frame, we can use the components of the force in the robot frame and the distance from the cog to the hinge point. When the angle between the robot and the tether is $(\psi_r, \theta_r, \phi_r)$ the length of normal from cog to tether force vector $d_n$ is:

$$ d_n = d_r\begin{bmatrix}\sin\psi_r\\\sin\theta_r\\\sin\phi_r\end{bmatrix} = d_r\begin{bmatrix}0\\\sin\theta_r\\0\end{bmatrix} = d_r\sin\theta_r \quad (10) $$

and the torque around the cog due to the tether force is:

$$ {}^{R}\tau_{teth} = \begin{bmatrix}\tau_x\\\tau_y\\\tau_z\end{bmatrix} = \begin{bmatrix}-d_{ny}f_{tethz} - d_{nz}f_{tethy}\\d_{nx}f_{tethz} - d_{nz}f_{tethx}\\-d_{ny}f_{tethx} + d_{nx}f_{tethy}\end{bmatrix} = \begin{bmatrix}-d_{ny}f_{tethz}\\0\\-d_{ny}f_{tethx}\end{bmatrix} \quad (11) $$

Forth, we equate them to the gravitational force, which always acts through the cog. The tether constrains the motion of the robot by opposing the force due to gravity and the torque produced by the fans. The motors move the robot by opposing the force due to gravity also.

$$ {}^{R}f_{g} = {}^{R}f_{fans} + {}^{R}f_{teth} \quad (12) $$

$$ {}^{R}\tau_{fans} = {}^{R}\tau_{teth} \quad (13) $$

The robot moves on a spherical shell at the end of the tether. It can swing out from the z axis of the reference frame and circle around the same axis. Stationary swing conditions occur when the robot has swung out from the axis but is not circling. In these conditions the force vector produced by the fans to achieve the force balance in Eqn. 12. intersects the this z axis.

### *B. Dynamics*

When there is a force imbalance, the resultant torque causes the robot to turn round its long axis and the force vector no longer intersects the z axis and the robot starts to circle. To maintain motion in a circle the fans have to supply a centripetal force $f_{cent}$ toward the z to balance the centrifugal force due to the circular motion.

$$ f_{cent} = \dot{\phi}^2\,{}^{R}d_{swing} \quad (14) $$

where $d_{swing}$ is the radius of the circle the robot is swinging around. This force is to be added to the force balance equation (Eqn. 12.).

Replacing the forces with equivalent forces through the cog results in torques around the cog that cause oscillation of the robot around the cog at a higher frequency than the pendulum motion. The torque balance around the short axis of the robot (y axis) causes the inclination of the robot to be different from the slope of the tether.

$$ {}^{R}\tau_{y} = I_{short}\,{}^{R}\ddot{\theta} = \frac{m}{12}\left(3r_c^2 + d_c^2\right){}^{R}\ddot{\theta} \quad (15) $$

where

$r_c$ is the radius of the cylinder model of the robot, and

$d_c = d_1 + d_2 + d_3$ is the length of the cylinder.

The angular acceleration of the robot around the y axis with respect to the robot frame is the sum of two components: the angular acceleration of the tether frame around the reference frame and the acceleration of the robot frame around the hinge frame. The former causes the robot to swing and the latter causes the robot to oscillate around the cog at a higher frequency than it is swinging.

The torque balance around the long axis of the robot causes its heading to change and hence the robot to fly in a circle.

$$ {}^{R}\tau_{z} = I_{long}\,{}^{R}\ddot{\phi} = \frac{mr_c^2}{2}\,{}^{R}\ddot{\phi} \quad (16) $$

## V. MODEL FOR SIMULATION

To simulate the robot we need to convert the above model of the tethered robot into a model for simulation. This involves rewriting the equations to express the outputs at any instant in time $t$ in terms of the inputs at the same instant in time. The inputs are the two motor forces, which are described with continuous functions of time.

$$ f_{lft} = f_1(time) \text{ and } f_{rft} = f_2(time) \quad (17) $$

The output is the location of the robot cog in 6 dof expressed as the values for $p_x$, $p_y$, $p_z$, $\psi$, $\theta$, and $\phi$. The torque produced by the difference in the ducted fan forces changes the heading of the robot. Rearranging Eqn. 16.

$$ {}^{R}\ddot{\phi} = \frac{2 * {}^{R}\tau_z}{mr_c^2} \quad (18) $$

Then the angular velocity and heading can be calculated

by integration using finite difference mathematics.

$$\dot{\phi}_t = \dot{\phi}_{t-1} + \ddot{\phi}_t \delta t \tag{19}$$

$$\phi_t = \phi_{t-1} + \dot{\phi}_t \delta t \tag{20}$$

The force difference between the ducted fans can also produce small rotations around the x axis of the robot. These torques need to be extracted from Eqn. 13 and included in the dynamics so that the angular acceleration around the x axis can be calculated. The simulation calculations require a value for the force in the cable. It is calculated from the force balance in Eqn. 12.

The application of force by the motors causes the robot to fly both out from the z axis of the reference frame and around it. Rearranging Eqn 15. Gives the angular acceleration of the robot around the y axis.

$${}^{R}\ddot{\theta} = \frac{12 * {}^{R}\tau_y}{m\left(3r_c^2 + d_c^2\right)} \tag{21}$$

Again, finite difference mathematics is used to calculate the angular velocity and swing angle.

The above angular accelerations are all calculated with respect to the cog. Next, we use the transform in Eqn. 1. to calculate the angular acceleration of the robot cog in world coordinates. Now we have the angular values for both the pendulum and wobble motions. We can use these to calculate the location of the robot cog.

From the angular accelerations we can calculate the angular velocities and the angles. From the angles and the length of the tether we can calculate the location of the robot at any instant in time *t* from its location at *t-1*.

## VI. Control Software

The software for the robot consists of two parts: host and embedded. The host software provides a user interface to control and monitor the robot (Fig. 7.). It is written in LabVIEW and runs on a Macintosh host. The host software communicates with the robot over a serial radio link.

The embedded software controls the motion of the robot in response to commands from the host and sends monitoring data to the host. It is written in PBasic and runs on a Parallax Basic stamp.

Individual components of the software have been tested. The next stage of the project is to test the integration of this into a control system for the robot. The integration software has been written but not fully debugged and tested.

Once software testing is complete, we will commence experimenting with sensor based control. Initially, we will focus on control of yaw using information from the magnetometer, the INS and the ultrasonic sensors.

Once control of yaw is stabilized, we will experiment with control of swing angle. The two-axis inclinometer will be used in combination with range measurements to calculate the swing angle. Finally, we will experiment with the control of circular flight.

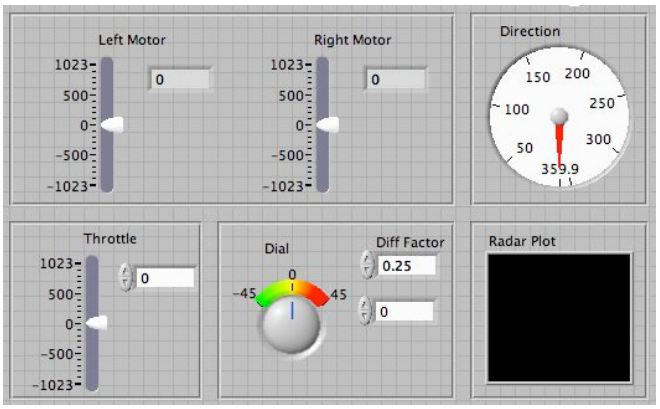


Fig. 7. LabVIEW user interface that enables control of motors or control of swing angle (Throttle) and heading.

## References


[1] D. Ratner, and McKerrow, P.J. "Aerial Tethered Robotic System With Hovering-Hopping Agents For Security and Rescue Operations", Proceedings AUVSI'06, Association for Unmanned Vehicle Systems International, August 29-31, Orlando, 2006. Won best paper award.

[2] Murphy, R.R., "Human-robot interaction in rescue robotics", IEEE Transactions on Systems, Man and Cybernetics, May 2004, Vol 34, No 2, pp 138-153.

[3] Messina, E. and Jacoff, A. "Performance Standards for Urban Search and Rescue Robots" Proceedings, SPIE Defense and Security Symposium, Orlando, April, 2006.

[4] Greer, G., McKerrow. P.J. and J. Abrantes, J. 'Robots in Urban Search and Rescue Operations', Proceedings ACRA'2002, Auckland, November, pp 25-30, 2002.

[5] Helble, H and Cameron, S. "OATS: Oxford Aerial Tracking System", Proceedings Towards Autonomous Robotic Systems, TAROS'06, Guildford, September 4-6, pp 72-79, 2006.

[6] Oh. P.Y. and Green, W.E., "CQAR: Close Quarter Aerial Robot Design for Reconnaissance, Surveillance and Target Acquisition Tasks in Urban Areas", International Journal of Computational Intelligence, Vol `, No 4, 2004, pp 353-360.

[7] McKerrow, P.J. 2004. Modelling the Draganflyer four-rotor helicopter, Proceedings ICRA'04, New Orleans, April, pp 3596-3601, 2004.

[8] Kumagai, J. Techno Cops, IEEE Spectrum, Vol 39, No 12, 2002, pp 34-39.

[9] Deng, X., Schenato, L. and Sastry, S.S. Attitude Control for a Micromechanical Flying Insect including Thorax and Sensor Models, ICRA 2003, Taipei, Taiwan.

[10] Oh. P.Y. and Green, W.E., " Mechatronic Kite and camera rig to rapidly acquire, process and distribute aerial images, IEEE/ASME Transactions on Mechatronics, December, 2004, Vol 9, No 4, pp 671-678.

[11] Yuh, J. "Design and control of autonomous underwater robots : A Survey", Autonomous Robots, Vol 8, No 1, January, 2000, pp 7-24.

[12] Krishna, M., Bares, J., Mutschler, E. "Tethering system design for Dante II, Proceedings ICRA, April, 1997, Vol 2, pp 1100-1105.

[13] Nohmi, M., Nenchev, D.V. and Uchiyama, M. "Tethered robot casting using a spacecraft-mounted manipulator, Journal of Guidance, Control, and Dynamics. Vol. 24, no. 4, pp. 827-833. July-Aug. 2001.

[14] de Oliveira, V.M. and Lages, W.F. "Predictive control of an underactuated brachiation robot using linearization, Proceedings 7th Portuguese Conference on Automatic Control, Lisboa, September, 2006.

[15] K. Usher, G. Winstanley, P. Corke, D. Stauffacher and R. Carnie, "A Cable-Array Robot for Air Vehicle Simulation", Proceedings Australasian Conference on Robotics and Automation, ACRA'04, 2004.

[16] McKerrow, P.J. "Introduction to Robotics", Addison-Wesley, Wokingham, ISBN 0 201 18240 8, 1991.